Cubic and orthorhombic structures of aluminum hydride AlH_3 predicted by a first-principles study

Xuezhi Ke,[1,*] Akihide Kuwabara,[2] and Isao Tanaka[2]
[1]*Fukui Institute for Fundamental Chemistry, Kyoto University, Kyoto 606-8103, Japan*
[2]*Department of Materials Science and Engineering, Kyoto University, Sakyo, Kyoto 606-8501, Japan*
(Received 23 January 2005; revised manuscript received 9 March 2005; published 25 May 2005)

The most stable structure of aluminum hydride AlH_3 is believed to be a hexagonal symmetry. However, using the density functional theory, we have identified two more stable structures for the AlH_3 with the cubic and orthorhombic symmetries. Based on the quasiharmonic approximation, the cubic and orthorhombic AlH_3 are almost degenerate when the zero-point energies are included. The geometric and electronic structures, the phonon, and the thermodynamic properties for the hexagonal, cubic, and orthorhombic AlH_3 have been studied by means of density functional theory and direct *ab initio* force constant approach. The calculated electronic structures, phonon density of states, and thermodynamic functions [including $S_{(T)}$ and $H_{(T)}-H_{(0)}$] for the three hydrides are similar. The results show that these three hydrides have negative enthalpies of formation, but positive free energies of formation. This conclusion is the same as that made by Wolverton *et al.* for the hexagonal AlH_3 [Phys. Rev. B **69**, 144109 (2004)]. The thermodynamic properties indicate that the orthorhombic and cubic AlH_3 should be more difficult to dissociate than the hexagonal AlH_3.

DOI: 10.1103/PhysRevB.71.184107 PACS number(s): 71.15.Nc, 61.66.Fn, 65.40.−b

I. INTRODUCTION

Aluminum hydride AlH_3 is a very important material since it has application as an energetic component in rocket propellants, a reducing agent in alkali batteries and polymerization catalysts, and a possible hydrogen source for fuel cells.[1,2] For the purpose of hydrogen storage, this material could be an excellent candidate if it can be cheaply produced, since it has a total capacity of 10 wt. % hydrogen, and hydrogen can be released upon heating to a little over 100 °C.[1] There are at least five AlH_3 phases found in the experiment.[2] Except for the hexagonal AlH_3, the crystal structures for the other phases are unknown. The experiment shows that both the thermal stability and ease of preparation of AlH_3 are strongly dependent on purity.[2] The hexagonal AlH_3 is the most stable structure so far isolated experimentally.[2] In addition, this hydride has been reported to be unstable in the presence of moisture or air, which may cause the structure to change or transform with time.[3] According to these reports, it seems that the presence of impurity or moisture affects the thermal stability of the hydrides significantly; therefore, it is natural to suspect that the hexagonal AlH_3 may be not a real ground-state structure. To explore this interesting problem, we chose some related compounds as the initial structures for this hydride, and then fully optimized them. Indeed, the orthorhombic and cubic AlH_3 are found to be more stable than the hexagonal AlH_3 in the present study.

Theoretically, only two references related to the aluminum hydride AlH_3 can be found so far.[4,5] In Ref. 4, the electronic structure for the hexagonal AlH_3 was discussed. In Ref. 5, the calculations show that this hydride has a small negative enthalpy of formation, but a large positive free energy of formation at $T=300$ K. Since the crystal structures for the other phases are unknown in experiment, to our best knowledge, there is no theoretical research on the properties of the orthorhombic and cubic AlH_3. In the current study, the orthorhombic and cubic AlH_3 have been identified, and have been found to be more stable than the hexagonal AlH_3. The enthalpy and free energy of formation among these three hydrides will be calculated in the temperature range from 0 to 500 K.

II. THEORETICAL METHODS

The quantum-mechanical calculations have been performed in the frame of density functional theory using the generalized gradient approximation (GGA),[6,7] as implemented in the VASP code.[8,9] The interaction between the ion and electron is described by the projector augmented wave method.[10] The cutoff energy for plane waves in our calculations is 600 eV. The configurations Al $3s^2 3p^1$ and H $1s^1$ are treated as the valence electrons. Brillouin-zone integrations are performed on the Monkhorst-Pack *k*-point mesh.[11] For each supercell, a high dense *k*-point mesh (spacing of *k*-points $<0.3/\text{Å}$) and a high plane wave cutoff energy of 600 eV are used. The total energy convergence within 0.5 meV per formula unit (f.u.) is well achieved. For example, for a supercell of $\sim 6.5\ \text{Å} \times \sim 6.5\ \text{Å} \times \sim 6.6\ \text{Å}$ (orthorhombic symmetry) a $5\times5\times4$ mesh is used. The total energy convergence within 0.3 meV/f.u. is achieved compared with either a more dense mesh of $11\times11\times9$ or a higher plane wave cutoff energy of 800 eV. Note that Wolverton *et al.* have demonstrated that the GGA is very suitable for the calculations of AlH_3.[5] Therefore, the GGA is used in our study.

In order to obtain the thermodynamic properties, one needs to know the phonon density of states (DOS). To calculate the phonon DOS, we use a direct *ab initio* force-constant approach implemented by Parlinski.[12] In this method a specific atom is displaced to induce the forces to act on the surrounding atoms, which are calculated via the

Hellmann-Feynman theorem. The forces are collected to construct the force-constant matrices. The dynamical matrices are then solved to obtain phonon frequencies. It should be noted that all anharmonic effects are omitted in this method. To check whether the anharmonicity is significant or not, we used two different displacements of 0.03 and 0.06 Å, and found that the results between these two cases are almost the same. For example, for the cubic AlH_3 the zero-point energy (ZP) difference between the two cases is within 1.5 mev/f.u., which is quite small. This indicates that the harmonic approximation is valid for these hydrides (at least for low temperatures).

III. RESULTS AND DISCUSSION

In this section, the geometric and electronic structures (in Sec. III A), the phonon density of states (in Sec. III B), the thermodynamic functions (in Sec. III C), and the enthalpy and Gibbs free energy of formation (in Sec. III D) for the hexagonal, orthorhombic, and cubic AlH_3 will be presented.

A. Geometric and electronic structures

To explore the crystal structure of aluminum hydride AlH_3, 60 types of the potential structures have been considered. They include: BF_3 [space groups, $P\bar{1}$ (see Ref. 13) and $P21/c$ (see Ref. 14)], BI_3 [space group $P\bar{6}3/m$ (see Ref. 15)], AlF_3 [space groups $Cmcm$,[16] P_4/nmm,[17] $R\bar{3}H$,[18] $P321$,[19] and $R32$ (see Ref. 20)], AlI_3 [space group $Pna21$ (see Ref. 21)], GaF_3 [space group $R\bar{3}c$ (see Ref. 22)], InF_3 [space group $R\bar{3}c$ (see Ref. 23)], TiF_3 [space groups $R\bar{3}mr$ (see Ref. 24) and $R\bar{3}c$ (see Ref. 25)], BiF_3 [space group $Fm\bar{3}m$ (see Ref. 26)], YH_3 [space group $P\bar{3}c1$ (see Ref. 21)], HoH_3 [space group, $P\bar{3}c1$ (see Ref. 27)], and AB_3 (A=F and I; B=Y, Fe, Re, etc.). For each structure, the cell volume and shape, and the atomic coordinates are fully optimized until the forces are less than 0.0001 eV/Å per atom. With these efforts, indeed, we found that the orthorhombic and cubic AlH_3 are more stable than the hexagonal AlH_3. The crystal structures for the hexagonal, orthorhombic, and cubic AlH_3 are shown in Fig. 1, and the lattice constants and coordinates are compiled in Table I. Figure 1 shows that the orthorhombic and cubic AlH_3 are more stable than the hexagonal AlH_3 by ~20 meV/f.u.. Note that this result is obtained on the basis of their equilibrium structures, and it may be slightly changed as the quasiharmonic approximation is adopted in the latter section. Also it should be noted that this result is obtained at the temperature 0 K. It is still not sure whether this is true at elevated temperature. We will discuss this issue by investigating thermodynamic properties in the latter section. For the hexagonal AlH_3, Table I shows that the calculated lattice constants are a=4.489 Å and c=11.820 Å, which are in very good agreement with the experimental values (a=4.449 Å and c=11.804 Å in Ref. 28) as well as the previous GGA calculations (a=4.42 Å and c=11.80 Å in Ref. 5). We do not find the experimental lattice constants for the other two hydrides.

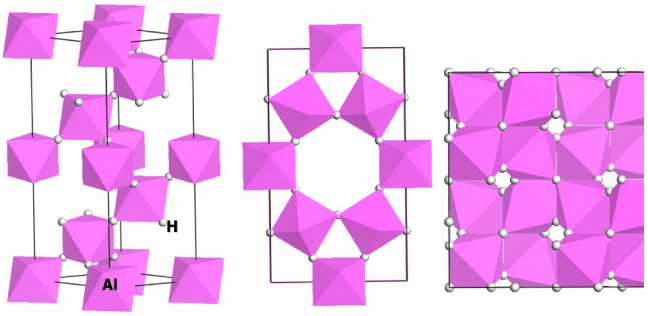

Hexagonal ($R\bar{3}c$)	Orthorhombic ($Cmcm$)	Cubic ($Fd\bar{3}m$)
E_{tot}= 0 meV/f.u.	E_{tot} = -19.3 meV/f.u.	E_{tot} = -32.4 meV/f.u.
E_{zp}= 0 meV/f.u.	E_{zp} = 2.1 meV/f.u.	E_{zp} = 6.4 meV/f.u.

FIG. 1. (Color online) Crystal structures for the hexagonal (on the left side), orthorhombic (in the middle), and cubic (on the right side) AlH_3. E_{tot} and E_{zp} represent the total energy and the zero-point energy of the optimized structure, respectively. E_{tot} and E_{zp} for the hexagonal AlH_3 are chosen as the zero reference energy. Small white balls represent hydrogen atoms, and Al atoms are located in the center of the cages.

The calculated electronic total and partial DOS for the hexagonal, orthorhombic, and cubic AlH_3 are presented in Figs. 2(a)–2(c), respectively. For the orthorhombic AlH_3, there are four nonequivalent hydrogen atoms (and two nonequivalent Al atoms) in the unit cell. Only one type of atom is plotted here since they differ only slightly. For the hexagonal AlH_3, the current total and partial (for hydrogen) DOS are similar to those recently calculated by Aguayo and Singh.[4] Overall, the total and partial DOS among these three hydrides are similar; i.e., the valence band of Al 3p character is almost the same level as that of H 1s (the curve shapes are also similar). This indicates that there may be a strongly covalent interaction between the Al and H atoms. However, some authors suggest that the bonding is mainly ionic in the hexagonal AlH_3.[4,29] To get a better understanding of this interaction, the bond overlap population (BOP) values are calculated on the basis of the Mulliken population. The BOP can provide useful information about the bonding property between the two atoms. A high BOP value indicates a strong covalent bond, while a low BOP value indicates an ionic interaction. The calculated results are compiled in Table II. Table II shows that the BOP values for the H–Al bonds among the three hydrides are 0.41–0.51. These values are greater than that (0.39) for the ionic H–Na bond in NaH, but smaller than those for the covalent H–Al bonds in $NaAlH_4$ (0.88) and Na_3AlH_6 (0.62~0.64).[30] Therefore, the H–Al bonds for these three hydrides are between the ionic and covalent interaction, and more close to ionic interaction to some extent. Since the bonding property and the bond length among these three hydrides are similar (see Table II for the bond length), their vibrational properties may be similar.

B. Phonon density of states (DOS)

The calculated phonon DOS for the hexagonal, orthorhombic and cubic AlH_3 are shown in Fig. 3. The solid, dashed, and dotted lines represent the DOS for the hexago-

TABLE I. Calculated lattice constants and fractional coordinates for the hexagonal, orthorhombic and cubic AlH_3. For the hexagonal AlH_3, the lattice constants are $a=b=4.489$ Å, $c=11.820$ Å, and $\gamma=120°$, and the fractional coordinates are Al (0, 0, 0) and H (0.6234, 0, 0.25). For the orthorhombic and cubic AlH_3, $\alpha=\beta=\gamma=90°$, and their coordinates are listed.

Orthorhombic AlH_3 (AlF_3 type) ($a=6.523$ Å, $b=11.139$ Å, $c=6.604$ Å)					Cubic AlH_3 (FeF_3 type) ($a=9.064$ Å)				
Atom	Site[a]	x	y	z	Atom	Site[a]	x	y	z
Al1	4*a*	0	0	0	Al	16*d*	0.5	0	0
Al2	8*d*	0.2500	0.2500	0.0000	H	48*f*	0.4306	0.1250	0.1250
H1	8*f*	0.0000	0.2862	0.9453					
H2	16*h*	0.1906	0.1024	0.0492					
H3	4*c*	0.0000	0.9571	0.2500					
H4	8*g*	0.2071	0.2853	0.2500					

[a]Wyckoff position.

nal, or thorhombic, and cubic AlH_3, respectively. For the hexagonal AlH_3, the current result is in good agreement with the previous calculations.[5] Since the mass of H atom is much smaller than that of Al atom, the high-frequency modes (above 12 THz) are dominated by the H atom, and the low-frequency modes (below 12 THz) are dominated by Al atoms. As a whole, the calculated phonon DOS among the three hydrides are similar. This indicates that their thermodynamic functions may not differ much.

C. Thermodynamic functions

The thermodynamic functions including the vibrational entropy $[S_{(T)}]$ and the internal energy $[E_{(T)}]$ are evaluated from the above calculated phonon DOS. $E_{(T)}$ is calculated by

$$E_{(T)} = \frac{1}{2} r \int_0^\infty \hbar\omega g(\omega) \coth\left(\frac{\hbar\omega}{2k_B T}\right) d\omega, \tag{1}$$

where $g(\omega)$ is the phonon DOS of the lattice, r is the number of degrees of freedom in the unit cell, $\hbar$ is the Planck constant, k_B is the Boltzmann constant, and T is the temperature. In the low-temperature limit, the internal energy is equal to the ZP energy:

$$E_{zp} = \lim_{T\to 0} E_{(T)} = \frac{1}{2} r \int_0^\infty \hbar\omega g(\omega) d\omega. \tag{2}$$

The Helmholtz free energy $[F_{(T)}]$ is calculated by,

$$F_{(T)} = E_{elec} + E_{(T)} - TS_{(T)}, \tag{3}$$

where E_{elec} is the electronic energy of the lattice obtained from the total-energy calculation. To obtain these functions, in practice, we use the quasiharmonic approximation,[31] i.e., the phonons are harmonic, but they are volume dependent. In detail, the cell volumes are expanded or compressed. For each volume, the cell shape and the atomic coordinates are fully optimized until the forces are less than 0.0001 eV/Å per atom. After that, the Helmholtz free energy is computed as a function of volume. The equilibrium volume at the temperature T can be obtained by minimizing the free energy. Once the $S_{(T)}$ and $E_{(T)}$ values are known, the enthalpy $[H_{(T)}]$ and the Gibbs free energy $[G_{(T)}]$ can be obtained by

$$H_{(T)} = E_{elec} + E_{(T)} + pV, \tag{4}$$

$$G_{(T)} = H_{(T)} - TS_{(T)}, \tag{5}$$

where E_{elec} is the electronic energy of the lattice obtained from the total-energy calculation, and p is the pressure (1 atm), and V is the volume.

The calculated entropy $[S_{(T)}]$ and enthalpy $[H_{(T)}-H_{(0)}]$ for the hexagonal, orthorhombic, and cubic AlH_3 are shown in Figs. 4(a) and 4(b), respectively. For the hexagonal AlH_3, both Figs. 4(a) and 4(b) show that the calculated data are in excellent agreement with the measured values.[32,33] For the hexagonal AlH_3, it is interesting to compare the current results with the previous calculations (see Ref. 5). Our calculated zero point for the AlH_3 (0.660 eV/f.u.) is good agreement with the previous result (0.644 eV/f.u.), and our calculated thermodynamic functions are also in good agreement with the previous calculations. As a whole, the calculated thermodynamic functions among the three hydrides are similar although the entropy for the orthorhombic AlH_3 is slightly greater than those for the hexagonal and cubic AlH_3.

For the fcc Al lattice, its thermodynamic functions are calculated also on the basis of the quasiharmonic approximation. The calculated enthalpy and Gibbs free energy for the Al lattice are shown in Figs. 5(a) and 5(b), respectively. The solid and dotted lines represent the calculated and measured results, respectively. Both Figs. 5(a) and 5(b) show that the calculated data agree well with the experimental results.[34] For the zero-point energy, the current result (0.037 eV/atom) is in good agreement with the previous calculation (0.040 eV/atom in Ref. 5).

For the H_2 gas molecule, the vibrations can not be treated directly from the phonon calculations because the phonon approach always considers the system as a solid (lattice), and thus neglects the translational and rotational vibrational modes. To obtain the thermodynamic functions of the H_2, we use the same procedure as that of Ref. 5. In detail, the H_2

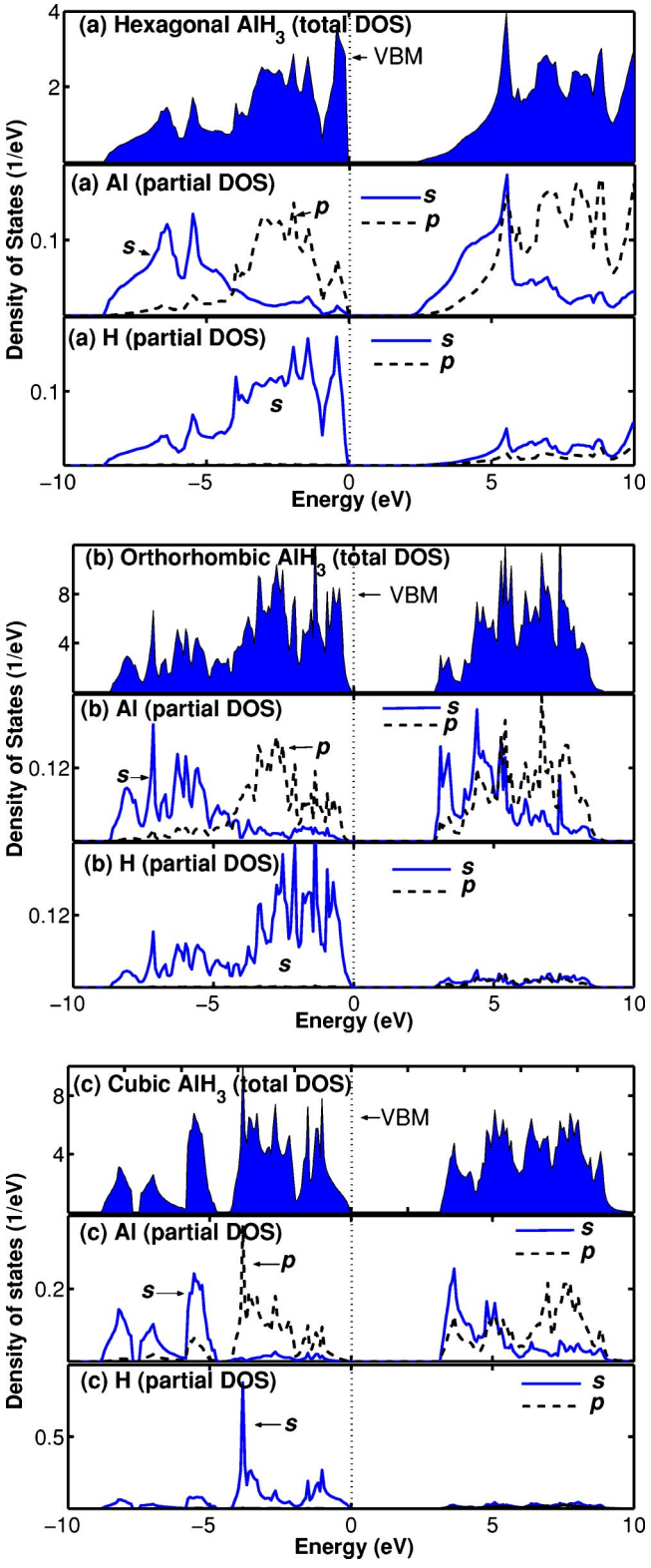

FIG. 2. Calculated electronic total and partial DOS for the hexagonal (a), orthorhombic (b), and cubic (c) AlH_3. For the orthorhombic AlH_3, there are four nonequivalent hydrogen atoms in the unit cell. Only one type of atom is plotted here since they differ only slightly. The valence band maximum (VBM) is denoted as the dotted line.

TABLE II. Calculated bond overlap population (BOP) and total charges for the hexagonal, orthorhombic, and cubic AlH_3.

Properties	Hexagonal AlH_3	Orthorhombic AlH_3	Cubic AlH_3
Bond length of H–Al	1.719 (Å)	1.718–1.720 (Å)	1.721 (Å)
BOP of H–Al	0.41	0.49–0.51	0.48
Total charge of Al atom	1.64	1.63	1.68
Total charge of H atom	1.45	1.45–1.48	1.44

molecule is modeled by putting a H_2 dimer in a simple cubic supercell with a lattice constant 10 Å. The Gibbs free energy $[G_{(T)}(H_2)]$ of the H_2 is calculated by combining both the calculations and the experimental results:

$$G_{(T)}(H_2) = E_{elec}(H_2) + E_{zp}(H_2) + \Delta G_{(T)}(H_2), \tag{6}$$

where $E_{elec}(H_2)$ is the electronic energy of a H_2 molecule obtained from the total-energy calculations, $E_{zp}(H_2)$ is the zero-point energy of a H_2 molecule obtained from the phonon calculations, and the term $\Delta G_{(T)}(H_2)$ is the temperature-dependent Gibbs free energy with respect to the temperature of 0 K. As a common procedure,[35] the $\Delta G_{(T)}(H_2)$ can be calculated by

$$\Delta G_{(T)}(H_2) = [H_{(T)}(H_2) - H_{(0)}(H_2)] - T \times [S_{(T)}(H_2) - S_{(0)}(H_2)], \tag{7}$$

where $H_{(T)}(H_2)$ and $H_{(0)}(H_2)$ are the enthalpies of the H_2 at the T and 0 K, respectively, and $S_{(T)}(H_2)$ and $S_{(0)}(H_2)$ are the entropies of the H_2 at the T and 0 K, respectively. These values [including $H_{(T)}(H_2)$ and $S_{(T)}(H_2)$] can be obtained from the thermochemical data.[36]

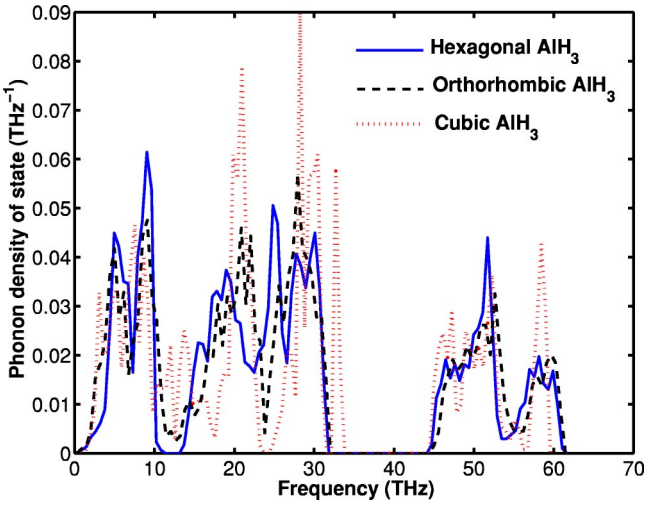

FIG. 3. Calculated phonon DOS for the hexagonal, orthorhombic, and cubic AlH_3. The solid, dashed, and dotted lines represent the DOS for the hexagonal, orthorhombic, and cubic AlH_3, respectively. The high-frequency modes (above 12 THz) are dominated by the H atom, and the low-frequency modes (below 12 THz) are dominated by Al atoms.

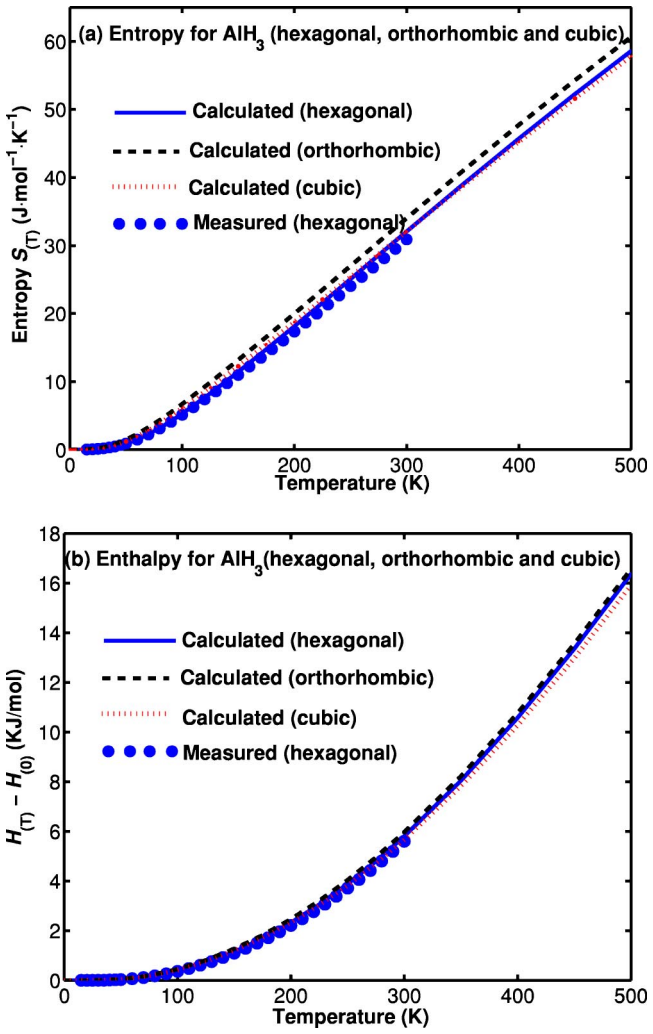

FIG. 4. Calculated thermodynamic functions for the hexagonal (solid line), orthorhombic (dashed line), and cubic (dotted line) AlH_3. The functions including the entropy $[S_{(T)}]$ and the enthalpy $[H_{(T)}-H_{(0)}]$ are presented in (a) and (b), respectively. $H_{(0)}$ denotes the enthalpy at 0 K. Dots are the measured data for the hexagonal AlH_3 (see Refs. 32 and 33).

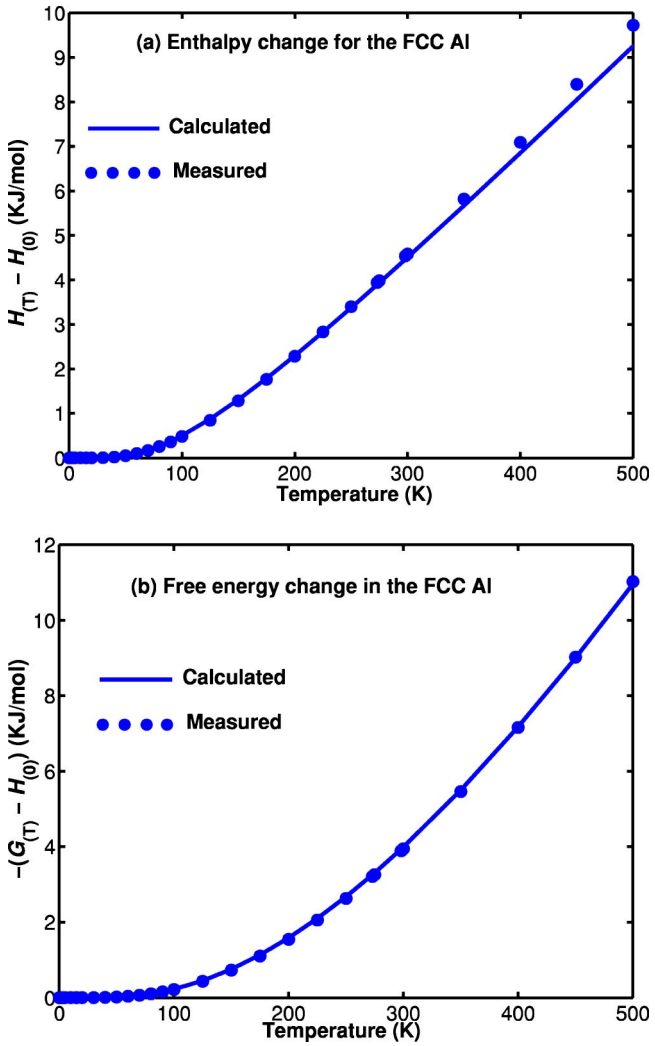

FIG. 5. Calculated and measured enthalpy (a) and Gibbs free energy (b) for the fcc Al lattice. The solid and dotted lines represent the calculated and measured results, respectively. The experimental data are from Ref. 34.

D. The enthalpy and Gibbs free energy of formation

Based on the above calculated thermodynamic functions, the enthalpy of formation and the Gibbs free energy of formation can be calculated. Concerning the formation energy, we consider the stability of AlH_3 with respect to decomposition into the fcc Al metal and the H_2 gas, i.e., the reaction

$$AlH_3 \rightarrow Al + \frac{3}{2}H_2, \tag{8}$$

where AlH_3 includes the hexagonal, orthorhombic and cubic symmetries. For convenience, we denote $a1 = AlH_3$ (hexagonal symmetry), $a2 = AlH_3$ (orthorhombic symmetry), $a3 = AlH_3$ (cubic symmetry), and $b = (Al + \frac{3}{2}H_2)$. The symbol ΔG_{a1-b} indicates that the free energy difference between the $a1$ and the b; i.e., $\Delta G_{a1-b} = G_{a1} - G_b$. The calculated enthalpy and Gibbs free energy of formation for the three hydrides are shown in Figs. 6(a) and 6(b), respectively. The solid, dashed, and dotted lines represent the data for the hexagonal, orthorhombic, and cubic AlH_3, respectively. For the hexagonal AlH_3 at the $T = 298$ K, the calculated enthalpy and Gibbs free energy of formation are −0.128 and 0.465 eV, respectively, which agree well with the experiment values[32] (-0.118 ± 0.009 and 0.482 ± 0.010 eV, respectively). These results are also in good agreement with the previous calculations (−0.072 and 0.516 eV, respectively; the GGA results in Ref. 5). Figure 6(b) shows that the Gibbs free energies of formation for these three hydrides are positive in the whole temperature range, indicating that they are unstable with respect to decomposition into $Al + \frac{3}{2}H_2$ under thermal equilibrium condition. On the other hand, Fig. 6(a) shows that the enthalpies of formation for these hydrides become more and more negative as the temperature increases. This means that the decomposition reactions are endothermic. Therefore, although these hydrides are unstable, they still can be stabilized kinetically. In fact, for the hexagonal AlH_3 it has been found not to decompose at an appreciable rate below the temperature 373 K (see Ref. 1). In both Figs. 6(a) and 6(b),

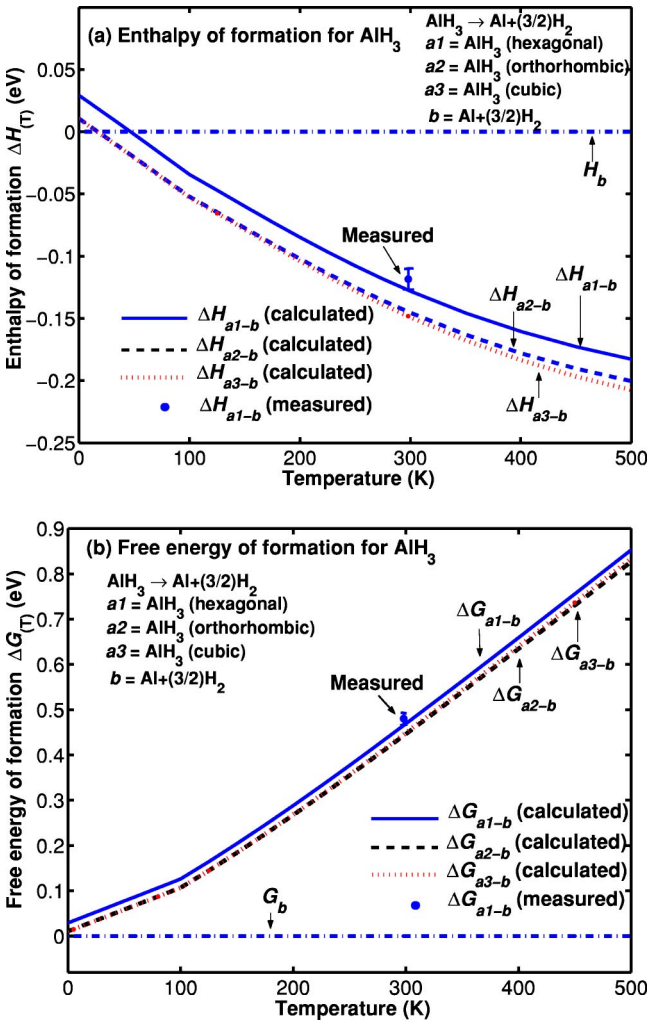

FIG. 6. Calculated enthalpy of formation (a) and Gibbs free energy of formation (b) for the hexagonal (solid line), orthorhombic (dashed line), and cubic (dotted line) AlH_3 as a function of temperature. For convenience, we denote $a1=AlH_3$ (hexagonal symmetry), $a2=AlH_3$ (orthorhombic symmetry), $a3=AlH_3$ (cubic symmetry), and $b=(Al+\frac{3}{2}H_2)$. The symbol of ΔG_{a1-b} indicates that the free energy difference between the $a1$ and the b; i.e., $\Delta G_{a1-b}=G_{a1}-G_b$. The energy of $(Al+\frac{3}{2}H_2)$ is chosen as the zero reference (denoted as a straight dashed-dotted line). Dots are the measured values for the hexagonal AlH_3 (see Ref. 32).

the dashed and dotted lines are always below the solid line, indicating that the orthorhombic and cubic AlH_3 are more stable than the hexagonal AlH_3 in the whole temperature range. Therefore, in principle, the orthorhombic and cubic AlH_3 should be more difficult to dissociate than the hexagonal AlH_3. This is meaningful for the purpose of hydrogen storage.

According to Figs. 6(a) and 6(b), we can see that the absolute values for the free energy of formation are much larger than those for the enthalpy of formation. This is due to the large entropy contribution ($T\Delta S$) from the H_2 gas. The entropy contributions for the $\frac{3}{2}H_2$ gas molecules, and the solid AlH_3 and Al lattices are shown in Fig. 7. Also for convenience, we denote $a1=AlH_3$ (hexagonal), $a2=AlH_3$ (orthorhombic), $a3=AlH_3$ (cubic), and $b=Al$ (fcc lattice).

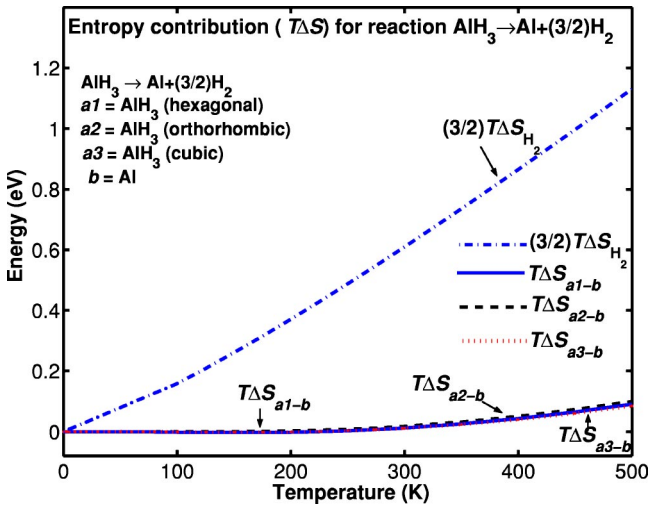

FIG. 7. Entropy contributions ($T\Delta S$) for the reaction of $AlH_3 \rightarrow Al+\frac{3}{2}H_2$. The contributions plotted here include the $\frac{3}{2}H_2$ gas, and the solid AlH_3 and Al lattices. For convenience, we denote $a1=AlH_3$ (hexagonal symmetry), $a2=AlH_3$ (orthorhombic symmetry), $a3=AlH_3$ (cubic symmetry), and $b=Al$ (fcc lattice). The term $\frac{3}{2}T\Delta S_{H_2}$ indicates the entropy contribution from the $\frac{3}{2}H_2$ gas molecules (denoted as a dashed-dotted line). The term $T\Delta S_{a1-b}$ indicates that the entropy contribution difference between the $a1$ and the b; i.e., $T\Delta S_{a1-b}=T\Delta S_{a1}-T\Delta S_b$. The $T\Delta S_{a1-b}$, $T\Delta S_{a2-b}$, and $T\Delta S_{a3-b}$ are denoted as solid, dashed, and dotted lines, respectively.

The term $\frac{3}{2}T\Delta S_{H_2}$ indicates that the entropy contribution for the $\frac{3}{2}H_2$ gas molecules. The term $T\Delta S_{a1-b}$ indicates that the entropy contribution difference between the $a1$ and the b; i.e., $T\Delta S_{a1-b}=T\Delta S_{a1}-T\Delta S_b$. Figure 7 shows that the entropy contribution $(\frac{3}{2}T\Delta S_{H_2})$ for the $\frac{3}{2}H_2$ molecules is significantly larger than those $(T\Delta S_{a-b})$ for the solids. Due to this large entropy contribution, and the relatively small negative enthalpy of formation for AlH_3 [see Fig. 6(a)], in fact, we found that the following reaction does not take place ever under the conditions of high pressure (up to 10 GPa) and low temperature (down to 0 K), as

$$Al+\frac{3}{2}H_2 \overset{\times}{\rightarrow} AlH_3, \tag{9}$$

where AlH_3 includes the hexagonal, orthorhombic, and cubic symmetries. This is consistent with the experimental observation,[1] in which the experiment found that the direct synthesis of AlH_3 through Eq. (9) does not occur under the conditions of hydrogen pressure 2.8×10^7 Pa and low temperature $-196\,^{\circ}C$ or hydrogen pressure 5.7×10^7 Pa and room temperature.

IV. SUMMARY

The geometric and electronic structures, the phonon, and the thermodynamic properties for the hexagonal, cubic, and orthorhombic AlH_3 have been studied by means of density functional theory and direct *ab initio* force constant approach.

Geometric structures. The most stable structure of alumi-

num hydride AlH_3 has been believed to be a hexagonal symmetry. However, in this study we have identified two new, and more stable structures for the AlH_3 with the cubic and orthorhombic symmetries. Although we cannot conclude that the cubic and orthorhombic AlH_3 are the ground-state structures, we think that our findings are interesting and fundamental. It may open a door for inspiring experimental efforts to find more stable AlH_3. The hexagonal AlH_3 is not the end.

Electronic properties. The electronic properties of the hexagonal, cubic, and orthorhombic AlH_3 have been discussed based on the electronic DOS, and the bond overlap population. The DOS indicates that there may be covalent interaction between the Al and H atoms. The further examination by the BOP analysis reveals that the H–Al bond is between the ionic and covalent interaction, and more close to the ionic interaction to some extent.

Phonon and thermodynamic functions. The calculated phonon DOS for the hexagonal, orthorhombic and cubic AlH_3 do not differ much. As a result, the thermodynamic functions for the three hydrides are almost the same. For the hexagonal AlH_3, the calculated entropy and enthalpy are in excellent agreement with experiment.

Enthalpy and Gibbs free energy of formation. For the hexagonal AlH_3, the calculated enthalpy and Gibbs free energy of formation agree well with experiment as well as previous calculations. The calculated free energies of formation for the hexagonal AlH_3 are positive in the whole temperature range, indicating that they are unstable with respect to decomposition into $Al+\frac{3}{2}H_2$; however, the calculated enthalpies of formation are negative, indicating that the decomposition reactions are endothermic. The conclusion is the same as that in Ref. 5 for the hexagonal AlH_3. For the orthorhombic and cubic AlH_3, we found that the situation is almost the same as that for the hexagonal AlH_3. As a result, although these hydrides are unstable, they still may be kept for a period of time because of the endothermic reactions. The calculated results indicate that the orthorhombic and cubic AlH_3 should be more difficult to dissociate than the hexagonal AlH_3. This may be meaningful for the purpose of hydrogen storage. Due to the large entropy contribution from the H_2 gas molecule, and the relatively small negative enthalpy of formation for AlH_3, this causes the direct syntheses of AlH_3 almost impossible even under the conditions of high pressure and low temperature.

ACKNOWLEDGMENTS

The authors thank Dr. T. Yamamoto, Dr. F. Oba, Dr. W. Bergermayer, and Dr. C. Wolverton for helpful discussion, and are grateful for the financial support of MEXT Japan on Computational Materials Science Unit in Kyoto University.

*Electronic address: ke@fukui.kyoto-u.ac.jp, xzke@yahoo.com

[1] *Hydrogen in Metals II*, edited by G. Alefeld and J. Völkl, Topics in Applied Physics Vol. 29 (Springer, Berlin, 1978).
[2] F. M. Brower, N. E. Matzek, P. F. Reigler, H. W. Rinn, C. B. Roberts, D. L. Schmidt, J. A. Snover, and K. Terada, J. Am. Chem. Soc. **28**, 2450 (1976), and references therein.
[3] M. Appel and J. P. Frankel, J. Chem. Phys. **42**, 3984 (1965).
[4] A. Aguayo and D. J. Singh, Phys. Rev. B **69**, 155103 (2004).
[5] C. Wolverton, V. Ozoliņš, and M. Asta, Phys. Rev. B **69**, 144109 (2004).
[6] J. P. Perdew and A. Zunger, Phys. Rev. B **23**, 5048 (1981).
[7] J. P. Perdew, J. A. Chevary, S. H. Vosko, K. A. Jackson, M. R. Pederson, D. J. Singh, and C. Fiolhais, Phys. Rev. B **46**, 6671 (1992).
[8] G. Kresse and J. Furthmüller, Comput. Mater. Sci. **6**, 15 (1996).
[9] G. Kresse and J. Furthmüller, Phys. Rev. B **54**, 11 169 (1996).
[10] P. E. Blöchl, Phys. Rev. B **50**, 17 953 (1994).
[11] H. J. Monkhorst and J. D. Pack, Phys. Rev. B **13**, 5188 (1976).
[12] K. Parlinski, Z-Q. Li, and Y. Kawazoe, Phys. Rev. Lett. **78**, 4063 (1997).
[13] Yu T. Struchkov, Yu A. Buslaev, A. M. Ellern, V. F. Sukhoverkhov, and Yu M. Antipin, Dokl. Akad. Nauk SSSR **279**, 892 (1984).
[14] D. Mootz and M. Steffen, Z. Anorg. Allg. Chem. **483**, 171 (1981).
[15] M. A. Ring, W. S. Koski, and J. D. H. Donnay, Inorg. Chem. **1**, 109 (1962).
[16] J. L. Fourquet, M. Leblanc, A. Lebail, H. Duroy, C. Jacoboni, and R. de Pape, J. Solid State Chem. **77**, 96 (1988).
[17] J. B. Parise, D. L. Thorn, G. A. Jones, J. A. Fernandez-Baca, N. Herron, T. Vogt, and R. L. Harlow, Chem. Mater. **7**, 75 (1995).
[18] D. Kissel and R. Hoppe, J. Fluorine Chem. **24**, 327 (1984).
[19] J. A. Ketelaar, Nature (London) **128**, 303 (1931).
[20] J. A. Ketelaar, Z. Kristallogr. **85**, 119 (1933).
[21] S. I. Troyanov, Zh. Neorg. Khim. **39**, 552 (1994).
[22] G. Garton, F. M. Brewer, and D. M. L. Goodgame, J. Inorg. Nucl. Chem. **9**, 56 (1959).
[23] C. Hebecker and R. Hoppe, Naturwiss. **53**, 104 (1966).
[24] P. Ehrlich and G. Pietzka, Z. Anorg. Allg. Chem. **275**, 121 (1954).
[25] S. Siegel, Acta Crystallogr. **9**, 684 (1956).
[26] U. Croatto, Gazz. Chim. Ital. **74**, 20 (1944).
[27] M. Mansmann and W. E. Wallace, J. Phys. (France) **25**, 454 (1964).
[28] J. W. Turley and H. W. Rinn, Inorg. Chem. **8**, 18 (1969).
[29] I. N. Goncharenko, V. P. Glazkov, A. V. Irodova, and V. A. Somenkov, J. Phys.: Condens. Matter **174**, 117 (1991).
[30] X. Ke and I. Tanaka, Phys. Rev. B **71**, 024117 (2005).
[31] A. A. Maradudin, E. W. Montroll, and G. H. Weiss, *Theory of Lattice Dynamics in the Harmonic Approximation*, 2nd ed. (Academic, New York, 1971).
[32] G. C. Sinke, L. C. Walker, F. L. Oetting, and D. R. Stull, J. Chem. Phys. **47**, 2759 (1967).
[33] K. S. Gavrichev, V. E. Gorbunov, S. I. Bakum, V. M. Gurevich, and A. D. Izotov, Inorg. Chem. **38**, 661 (2002).
[34] D. A. Ditmars, C. A. Plint, and R. C. Shukla, Int. J. Thermophys. **8**, 621 (1987).
[35] K. Reuter and M. Scheffler, Phys. Rev. B **65**, 035406 (2001).
[36] D. R. Stull and H. Prophet, *JANAF Thermochemical Tables*, 2nd ed. (U.S. National Bureau of Standards, Washington, DC, 1971).